Nuclear Instruments and Methods in Physics Research A 862 (2017) 8–17

Contents lists available at ScienceDirect

Nuclear Instruments and Methods in Physics Research A

journal homepage: www.elsevier.com/locate/nima

Fabrication and testing of a 4-node micro-pocket fission detector array for the Kansas State University TRIGA Mk. II research nuclear reactor

Michael A. Reichenberger [a,*], Daniel M. Nichols [a], Sarah R. Stevenson [a], Tanner M. Swope [a], Caden W. Hilger [a], Troy C. Unruh [b], Douglas S. McGregor [a], Jeremy A. Roberts [a]

[a] S.M.A.R.T. Laboratory, Mechanical and Nuclear Engineering Dept., Kansas State University, Manhattan, KS 66506, USA
[b] Idaho National Laboratory, Idaho Falls, ID 83415-3531, USA

ARTICLE INFO

Article history:
Received 27 January 2017
Received in revised form
10 April 2017
Accepted 29 April 2017
Available online 8 May 2017

Keywords:
Micro-Pocket Fission Detector
MPFD
In-Core Flux Monitor
Reactor Instrumentation

ABSTRACT

Advancements in nuclear reactor core modeling and computational capability have encouraged further development of in-core neutron sensors. Micro-Pocket Fission Detectors (MPFDs) have been fabricated and tested previously, but successful testing of these prior detectors was limited to single-node operation with specialized designs. Described in this work is a modular, four-node MPFD array fabricated and tested at Kansas State University (KSU). The four sensor nodes were equally spaced to span the length of the fuel-region of the KSU TRIGA Mk. II research nuclear reactor core. The encapsulated array was filled with argon gas, serving as an ionization medium in the small cavities of the MPFDs. The unified design improved device ruggedness and simplified construction over previous designs. A 0.315-in. (8-mm) penetration in the upper grid plate of the KSU TRIGA Mk. II research nuclear reactor was used to deploy the array between fuel elements in the core. The MPFD array was coupled to an electronic support system which has been developed to support pulse-mode operation. Neutron-induced pulses were observed on all four sensor channels. Stable device operation was confirmed by testing under steady-state reactor conditions. Each of the four sensors in the array responded to changes in reactor power between 10 kWth and full power (750 kWth). Reactor power transients were observed in real-time including positive transients with periods of 5, 15, and 30 s. Finally, manual reactor power oscillations were observed in real-time.

1. Introduction

The development of neutron detectors designed for high neutron-flux environments is important to support nuclear power research [1–3]. Micro-Pocket Fission Detectors (MPFDs) are a small, robust neutron sensor capable of real-time, in-core neutron-flux measurement [4–8]. MPFDs can be deployed along with experimental nuclear assemblies and into small cavities within research nuclear reactors because of their small size and low sensitivity.

The current generation of MPFDs utilize a multi-wire design wherein a thin (< 1 μm-thick) fissile layer is situated within an ionization chamber, bordered by two parallel wires, illustrated in Fig. 1. The parallel wires act as anode and cathode of the ionization chamber. An applied bias between the anode and cathode wires causes charge motion within the ionization chamber, measured using a charge-sensitive pre-amplifier. MPFDs are constructed of radiation hard, temperature resistant materials, thereby improving the durability of the sensor in high-flux and high-temperature experiment conditions [8]. Multiple MPFD sensors can be fabricated into an array to provide multiple measurement points in a single instrument.

Previous MPFD designs required the fabrication of the sensor array in conjunction with an extension cable coupled to single-channel electronics. A new MPFD fabrication and deployment method was developed to support research projects deploying MPFD arrays into nuclear reactor cores. The data from such three-dimensional MPFD arrays will be used to enhance reactor material experimentation and certification, and will be used to benchmark nuclear reactor simulations. First, a modular MPFD array was designed, consisting of four MPFD sensors separated by insulating silica spacers. The MPFD array was encapsulated in a straight, 6-foot long, stainless-steel tube. The individual MPFD sensors were distributed within the tube to cover the fuel region of a TRIGA fuel rod. The entire tube was filled with argon gas which can circulate into and out of each MPFD sensor, thereby reducing the potential for fission fragment saturation in the gas chambers. A vacuum and gas

* Correspondence to: S.M.A.R.T. Laboratory, Mechanical and Nuclear Engineering Dept., Kansas State University, 3002 Rathbone Hall, 1701B Platt Street, Manhattan, KS 66506, USA.
E-mail address: mar89@ksu.edu (M.A. Reichenberger).

http://dx.doi.org/10.1016/j.nima.2017.04.047
0168-9002/

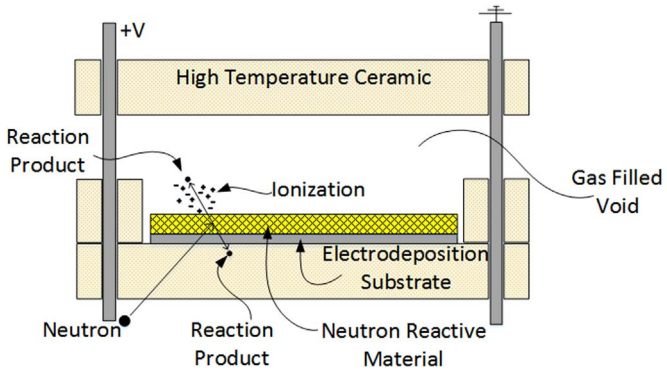

Fig. 1. Fission interactions in the fissile layer produce energetic fission fragments which deposit more energy in the ionization chamber than from other radiation interactions in the chamber [6].

fill assembly was fabricated at the top of the MPFD array to facilitate the purge of the tube and back-fill with high-purity ionization gas. An electrical plug at the top of the array connected the anode and cathode wires of each sensor to a commercially available extension cable. A commercially available electronics package was also used for pulse-processing [9]. This modular design improved the robustness of the MPFD instrument assembly by reducing the failure modes of the assembly. This shorter MPFD array also reduced the likelihood of failure in the array during fabrication and transportation to the test facility. The first modular MPFD array was constructed and tested in-core, yielding a stable response to reactor power and successfully tracking reactor transients.

Table 1
Alpha spectrometry was used to measure the activity, and subsequently the mass of uranium deposited onto each sample.

MPFD Node	Uranium Mass (μg)
1 (top of array)	0.533 ± 0.023
2	0.630 ± 0.026
3	0.548 ± 0.025
4 (bottom of array)	0.619 ± 0.014

2. Sensor fabrication

The disks and spacers that comprise each MPFD node for the modular array were each produced by slicing sections of hard-fired, extruded alumina into 0.040-in. (1-mm) thick units with a diamond wire saw. The individual samples were then processed by NUCFIL, LLC dba NFT® [10]. The faces of the disks were subsequently polished using an extra fine grit diamond polishing paste applied to a smooth surface for hand lapping. The spacers have a 0.040-in. (1-mm) wide, 0.020-in. (0.5-mm) deep trench across two wire holes as shown in Fig. 2. The trench connecting

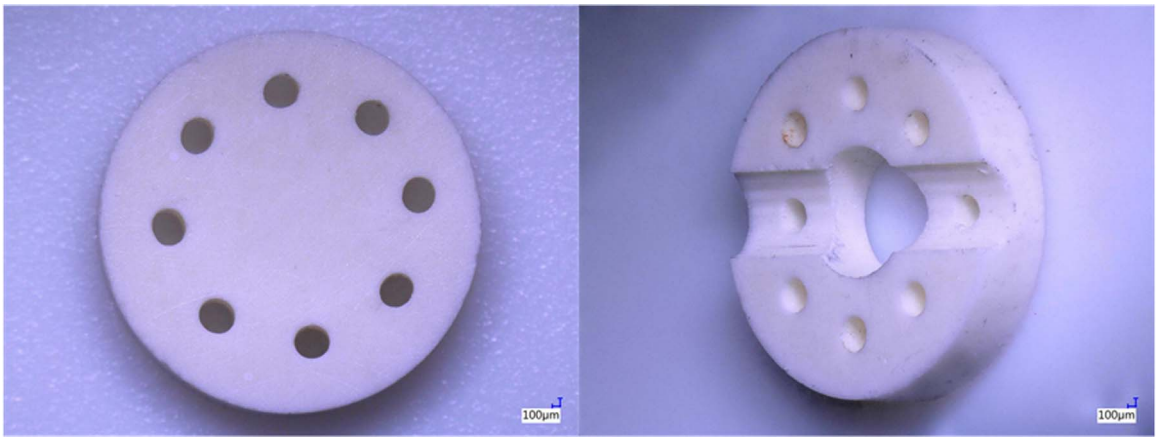

Fig. 2. Each MPFD node was composed of two disks (example on left) and two spacers (example on right) creating the ionization chamber with a channel exposing the appropriate anode and cathode wires.

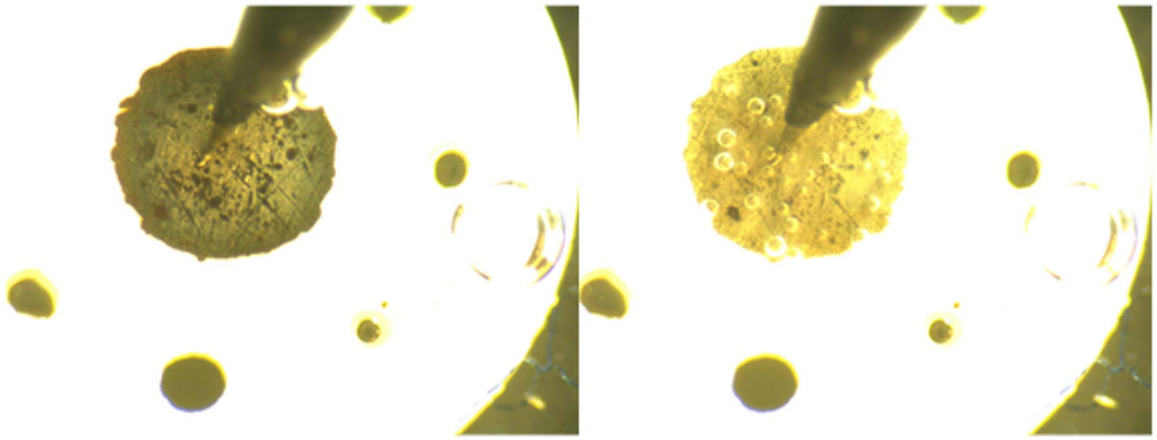

Fig. 3. The uranium was clearly visible on the surface of each substrate during the electrodeposition process. The uncoated sample appeared grey (left) while the coated sample was appeared yellow (right) from the presence of the uranium compound. (For interpretation of the references to color in this figure legend, the reader is referred to the web version of this article.)

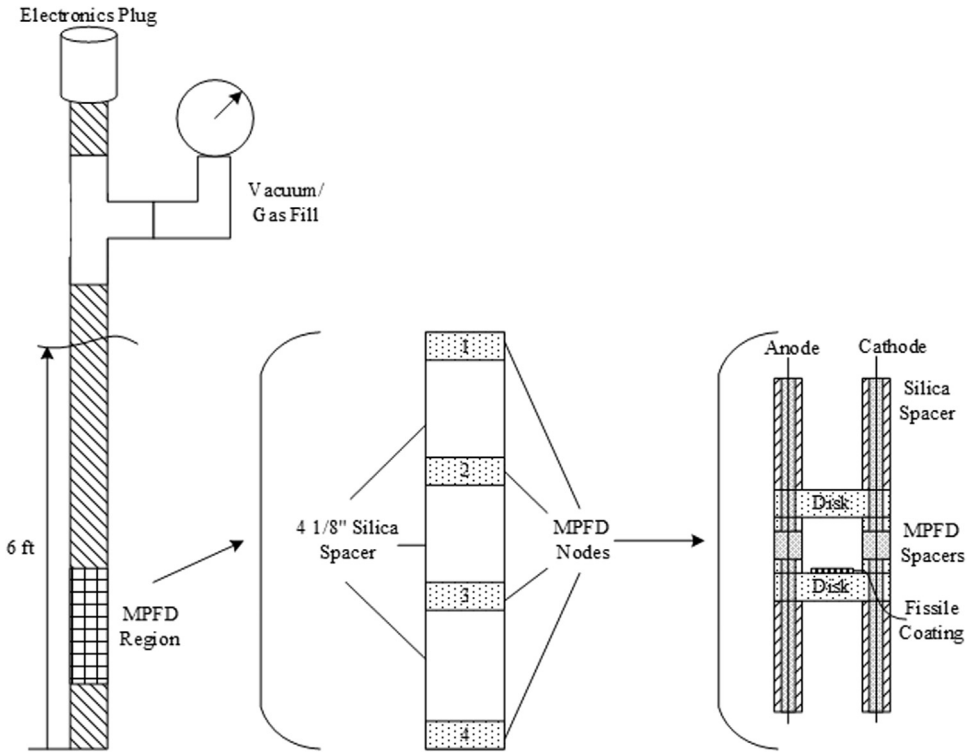

Fig. 4. The modular MPFD array included four MPFD nodes distributed near the bottom of a 6-foot long stainless steel tube which was purged, back-filled with argon gas, and sealed.

the electrode holes was used to provide a path for charge carriers to travel within the ionization chamber of the MPFD as previously described.

Electrodes 0.060-in. (1.5 mm) in diameter were evaporated onto each of the polished disks, consisting of a 50 Å Ti adhesion layer and 500 Å Pt electrode. Electrodeposition of natural uranium followed [11]. The sample appeared grey prior to electrodeposition and rapidly changed to yellow during the electrodeposition process, shown in Fig. 3.

X-ray fluorescence confirmed the presence of uranium on each sample. The uranium mass was measured with alpha spectrometry; the amount on each of the four disks is summarized in Table 1. The variation in sample mass is most likely due to variations in the evaporated surface area of each sample.

After the uranium electrodeposition and analysis, assembly of the MPFD was initiated. The design of the array and sensor region are illustrated in Fig. 4. A single $0.3125 \times 0.020 \times 72$ in. 316 stainless steel tube was used to house the MPFD assembly to fit within the 0.315-in. (8-mm) diameter penetrations in the upper grid plate of the KSU TRIGA Mk. II research nuclear reactor [12]. A 316 stainless steel plug was welded onto the end of the tube, capping the end which penetrated the top grid-plate, which then rested on the bottom grid plate of the KSU TRIGA Mk. II reactor. Each MPFD node was composed of two disks and two spacers; however, only one disk was electrodeposited with fissile material. The two spacers were aligned such that the trenches formed a single 0.040-in. (1-mm) deep x 0.040-in. (1-mm) wide channel connecting one pair of opposing anode and cathode wires, illustrated in Fig. 4. Each MPFD sensor was indexed in order to dedicate a separate anode/cathode pair for each node.

The MPFDs were each separated by a 4.125-in. long silica spacers, as shown in Fig. 5. The total distance between each MPFD was therefore 4.375 in., including the thickness of the MPFD. Additional silica insulation was added beneath the MPFD region to separate the bottom MPFD (node 4) 7 in. from the bottom of the exterior of the encapsulation tube, illustrated in Fig. 6. In this manner, the four MPFD sensors were equally distributed within the fuel region of a typical TRIGA fuel rod at distances 7.188, 11.5623, 15.938, and 20.25 in. from the bottom of the array.

Following the assembly of the MPFD region, additional silica insulation was added to the array, isolating each anode and cathode wire and providing structural support for the wires within the encapsulation tube. The 30 AWG alumel anode and cathode wires were kept straight and separated during the assembly process to prevent damage to the wires. The crushable silica insulation was designed with a central hole, resembling the cross section of the spacer depicted in Fig. 2. This particular geometry was chosen to increase the volume of gas within the encapsulation tube and decrease the total capacitance of the array. Silica was chosen because of its low relative permittivity (between 3 and 4) compared to other mineral insulation (≈ 10).

The silica insulation extended the entire length of the stainless steel encapsulation tube, beyond which fiberglass insulation was used to insulate each electrode wire. Flexible fiberglass insulation was necessary to allow for the assembly of the gas purge/fill system and electrical feedthrough plug, as shown in Fig. 7. The vacuum/fill assembly was mounted next to the electronic plug to allow the anode and cathode wires to pass out of the encapsulation tube through the electronics plug.

Prior to final assembly, each anode and cathode was soldered to the appropriate pin of a FGG.1 K.308.CLAK80 Lemo® plug [13]. Each anode and cathode was confirmed to correspond to the correct MPFD node prior to final assembly. The respective PHG.1 K.308. CLLK75 Lemo® receptacle [14] was connected to the Belden 8134E extension cable [15], providing a connection between the modular MPFD array and the electronics. The fully-assembled array measured over 6 feet long due to the gas purge/fill assembly and electronic feedthrough. The materials at the top of the array were located sufficiently far from the top of the reactor core to minimize the effect of neutron irradiation (both activation and material degradation).

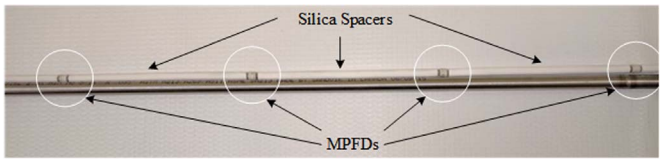

Fig. 5. Four MPFD nodes were constructed with 4.125-in. long silica spacers between each node. The total distance between the node center points was 4.375 in. due to the length of each MPFD node.

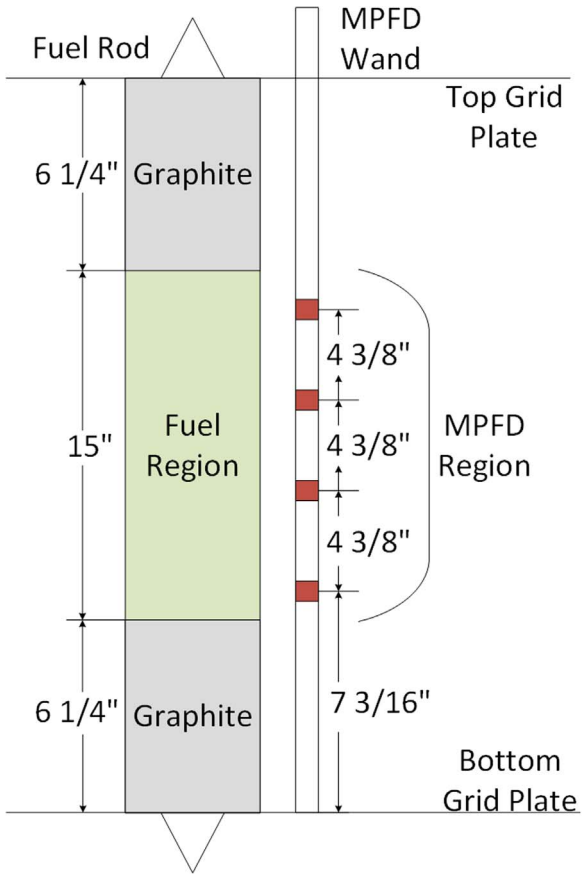

Fig. 6. The MPFD nodes were distributed evenly along the length of the fuel region of the core.

Ceramic materials can absorb water moisture when exposed to air, changing the electrical properties of the material. A low-temperature bake-out furnace was constructed to bake humidity out of the MPFD array. A 20-foot long silicone heating tape was wrapped around a 1-in. diameter copper pipe and insulated by 1.5-in. thick fiberglass insulation. The heat-tape is capable of temperatures up to 450 °C; however the tape was used on its lowest setting to achieve approximately 175 °C in the center of the pipe. A rough vacuum pump was connected to the purge system and allowed to pull a vacuum while at an elevated temperature for 24 h in order to remove humidity from within the array. After the heated vacuum purge was completed, the tube was filled to 30 psig with ultra-high-purity argon (UHPAr). The purge and gas fill process were repeated two additional times. After the array was filled a third time, the final assembly was complete and the array was ready to deploy in the KSU TRIGA Mk. II research nuclear reactor. The capacitance of each node was measured between 350 pF and 400 pF, including a 25-foot long extension cable (11 pF/ft) [15].

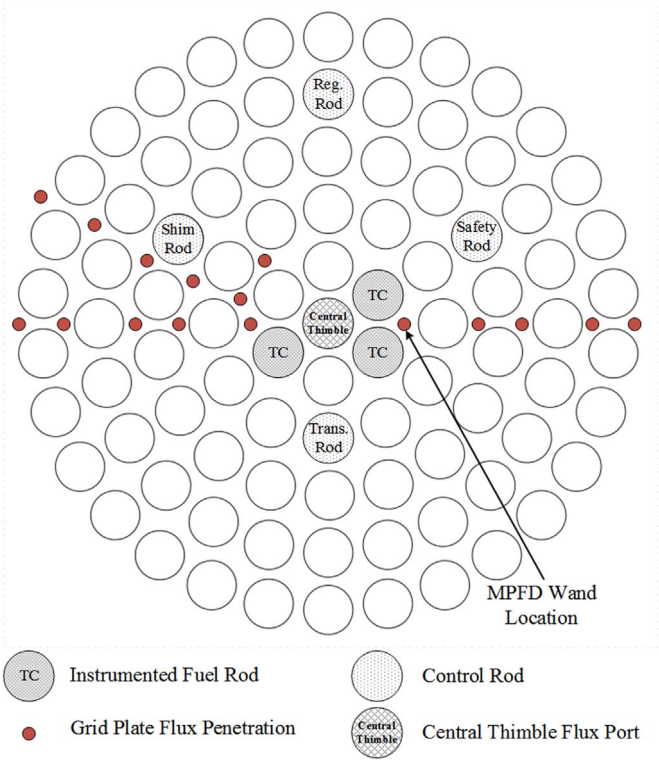

Fig. 8. The flux penetration between two instrumented fuel assemblies was chosen for close proximity to the center of the core and access to fuel temperature data.

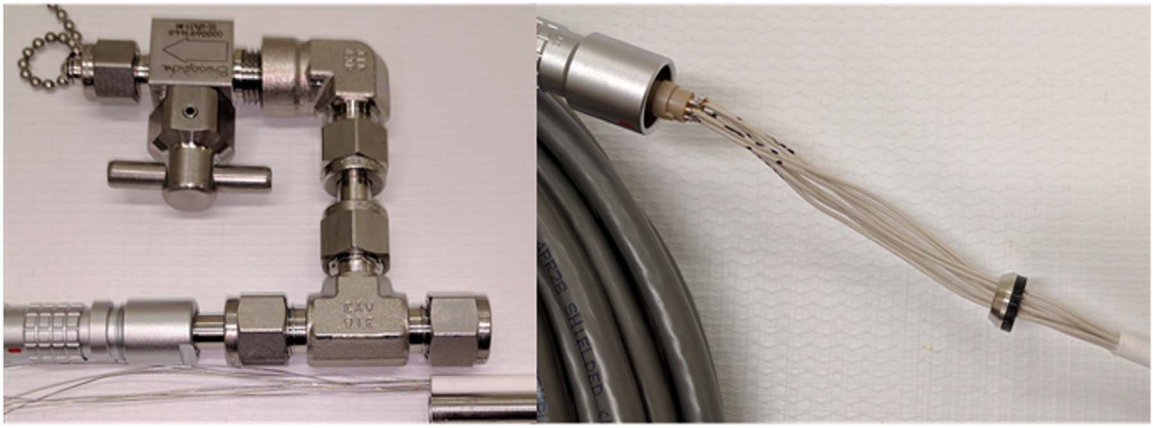

Fig. 7. The silica insulation was used throughout the length of the stainless-steel encapsulation tube.

3. Experimental Procedure

Prior research required the modification of the KSU TRIGA Mk. II research nuclear reactor upper fuel grid plate to include fifteen 0.315-in. (8-mm) diameter penetrations at locations illustrated in Fig. 8 [12]. The location situated between two instrumented fuel rods was chosen for testing of the 4-node encapsulated MPFD array, as shown in Fig. 8. The neutron flux near the center of the core is greater than the neutron flux extending radially outward. Therefore, MPFD response should be greatest in the center of the core, enhancing the data acquisition rate.

The electronic support system for the MPFD array included an MPR-16 preamplifier, MSCF-16 shaping amplifier with leading edge discrimination, a Philips Scientific 726 signal translator, NIMBox digital I/O unit, and custom LabView interface. The MPR-16 was set to 20 MeV mode, and the entire support system was tested with the MPFD emulator [9]. Emulated pulses were observed with a pulse amplitude of approximately 500 mV using an MSCF-16 shaping time of 0.25 μs and a gain of 10. Then, the MPFD array (still located outside of the reactor pool) was connected to the MPR-16 with the cable shield connected to the input ground. High voltages of +10 V, +100 V, +200 V, and +400 V were applied to the array, checking for high-voltage power supply (HVPS) current draw and increased noise on the oscilloscope. No additional noise was observed during out-of-core testing, and the HVPS current draw remained constant at <0.005 μA. The electronics were then powered off and the array was inserted manually into the flux port, shown in Fig. 9. The electronics were re-enabled and a +200 V bias was applied to the array. HVPS current and noise were monitored to ensure that no current flowed between anode and cathode wires. The reactor was then raised to 10 kWth with reactor cooling pumps off, eliminating noise from the electromechanical pumping system.

4. Experimental results

The objectives of in-core testing of the MPFD array included identification of neutron-induced pulses, confirmation of channel independence (no cross-talk), sensor response linearity with

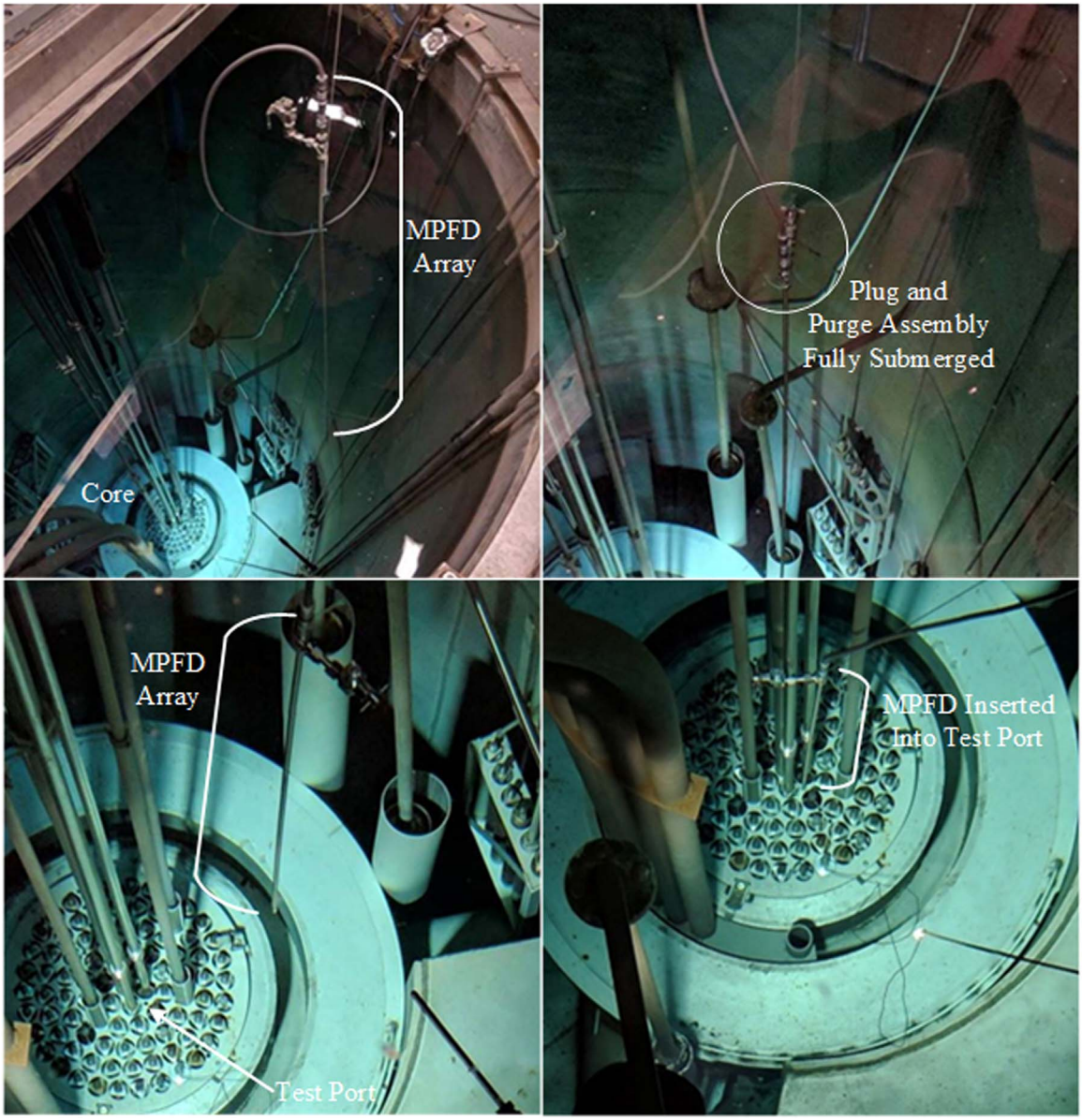

Fig. 9. A string was used to lower the array into the reactor pool, reducing stress on the wire connection. The MPFD array was inserted through the 0.315-in. (8-mm) diameter grid plate penetration into the reactor core.

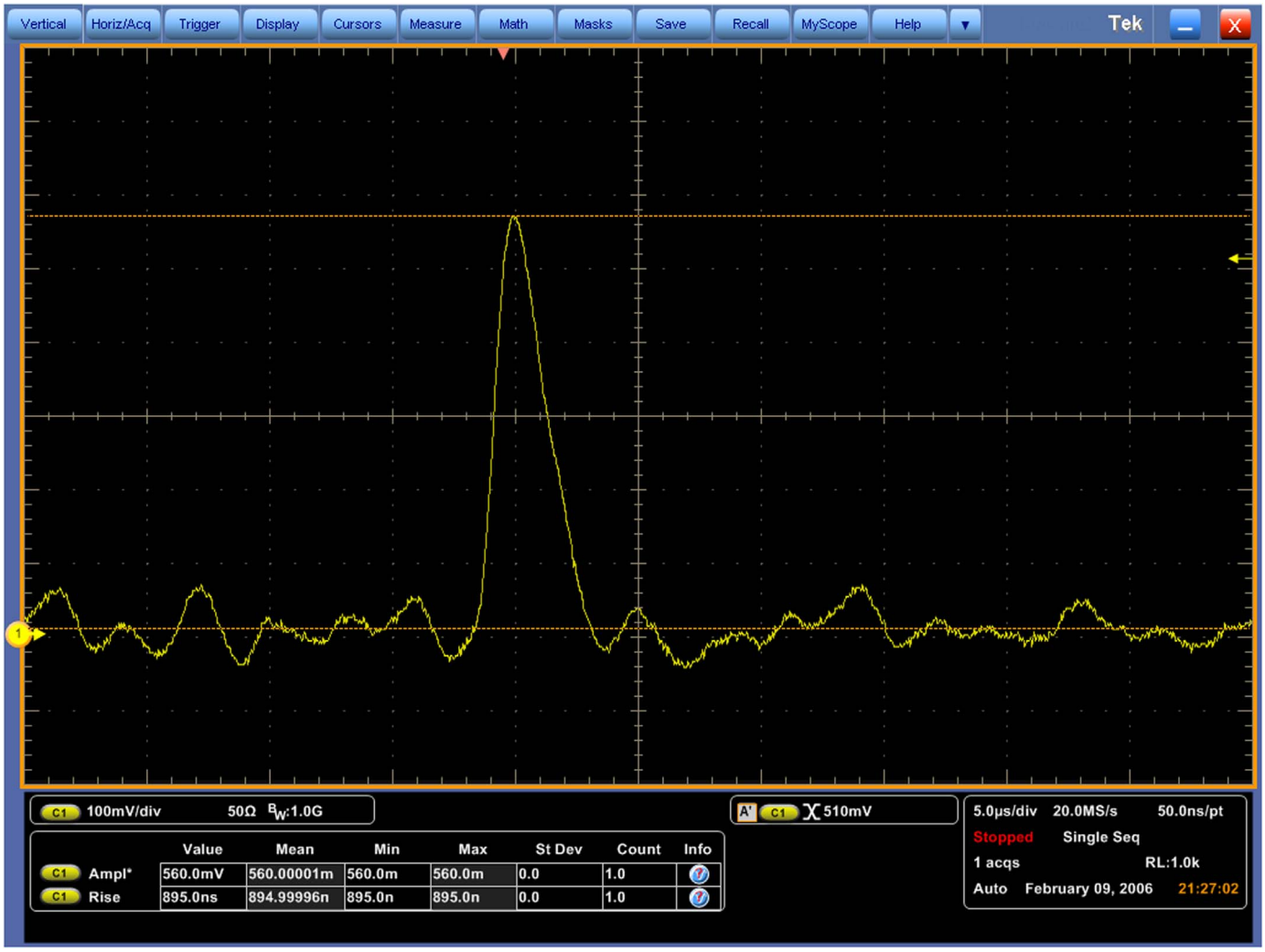

Fig. 10. Neutron pulses were first observed using the MPR-16 preamplifier in 20 MeV mode and with the MSCF-16 gain of 10 and shaping time of 0.5 μs.

reactor power, and real-time tracking of reactor power transients. The functionality of the MPFD array was tested at reactor powers above 10 kWth. The measurement frequency was also tested using 1 ms, 100 ms, and 1 s intervals to demonstrate the real-time data acquisition capabilities of the MPFD system.

4.1. Detector pulses

While the reactor was increasing in power, neutron-induced pulses were observed. After establishing criticality at 10 kWth, stability testing and neutron-induced pulse observation commenced. Using an MPR-16 preamplifier in 20 MeV sensitivity mode with an MSCF-16 amplifier shaping time of 0.25 μs and gain of 10, high-frequency noise was observed. The shaping time was increased to 0.5 μs to eliminate the high-frequency noise. A representative neutron-induced pulse, shown in Fig. 10, triggered the discrimination threshold of 15 on the MSCF-16, producing a >500 mV pulse. The pulse amplitude varied slightly, however, the average pulse amplitudes were consistently above the electronic noise observed to be under 100 mV.

The potential for cross-talk was a concern for multi-sensor MPFD arrays mainly because of the close proximity of the electrodes which carry voltage pulses. It is possible for such parallel wires to induce a voltage pulse across channels if the wires are sufficiently close and the signal sufficiently large. Each channel of the modular MPFD array was used to trigger the oscilloscope while all four channels were monitored simultaneously. Cross-talk could then be identified if coincident pulses were observed on multiple channels. In fact, no correlated pulses were observed. Two pulses are shown in Fig. 11 on different channels without noticeably perturbing the signal on other channels.

The stability of the detector array was also in question based on previous experiments which produced unstable or unreliable response rates after extended testing [8]. A custom LabView® interface was developed which counted the digital pulses produce by the electronic support system whenever a neutron interaction produced a pulse which exceeded the discrimination threshold. Approximately an additional 1% counting error was introduced by the counting system which did not utilize a synchronized timer. The modular MPFD array was tested at 10 kWth for 20 min, and had a stable response as shown in Fig. 12. The average mass-normalized response rate for each MPFD sensor is summarized in Table 2. The mass-normalized response rate for nodes 1 and 4 should be relatively close because of the symmetric nodal spacing in the fuel region of the reactor. The error from the mass measurement reported in Table 1 increased the uncertainty of the mass-normalized results beyond standard counting error. The mass-normalized response rates for channels 1 and 4 are indeed within 2σ of one another. Similarly, nodes 2 and 3 should have similar mass-normalized response rates. Channel 3 responded at a much higher rate than channels 1, 2, and 4. It is possible that the mass measurement of node 3 was incorrect, or that the

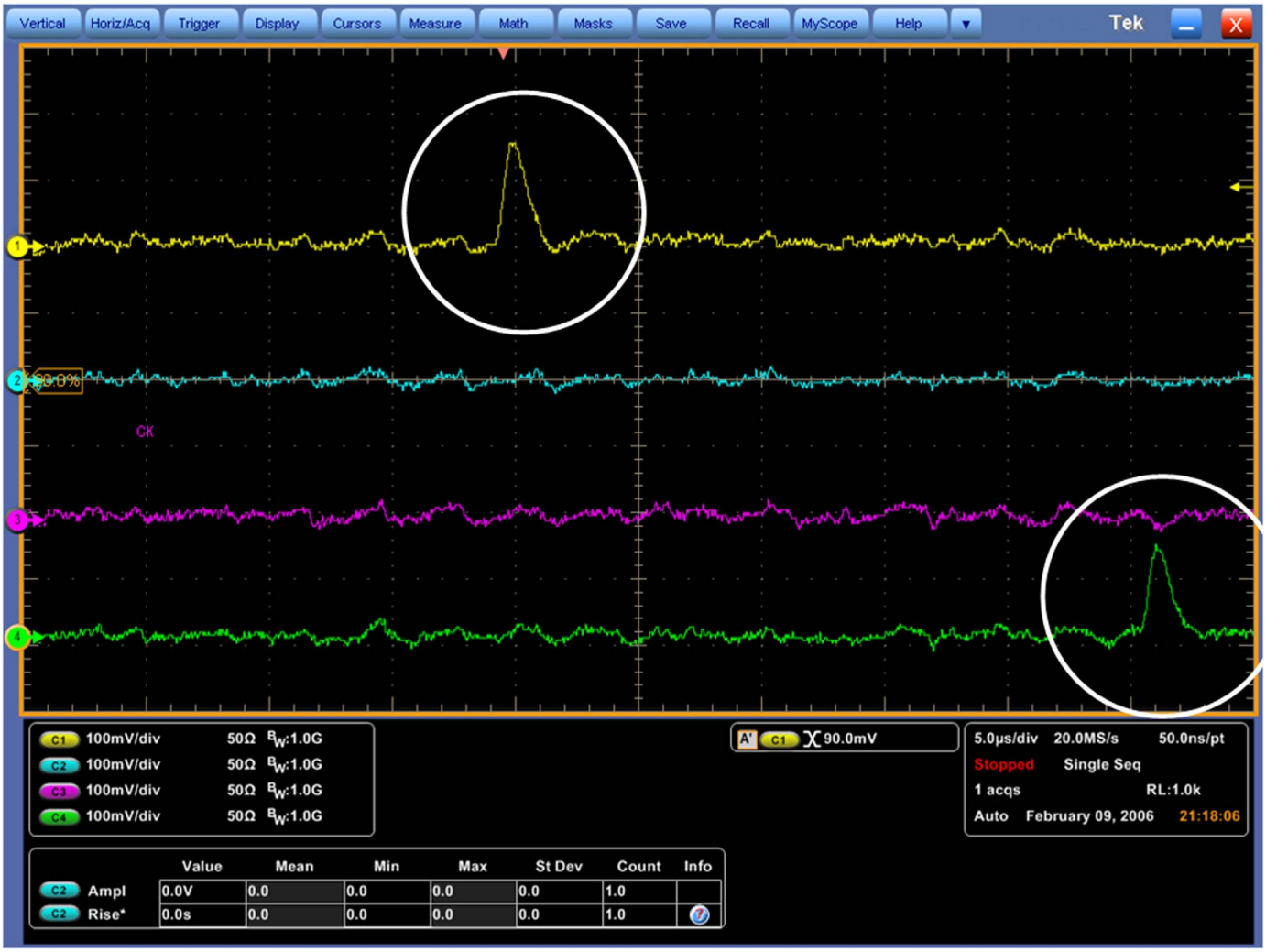

Fig. 11. Cross-talk was not observed between MPFD channels. Independent interactions could be observed on multiple channels at different times.

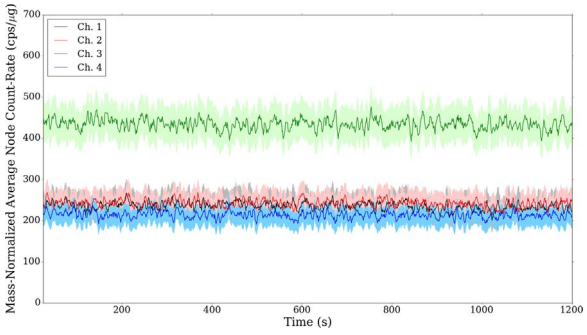

Fig. 12. The MPFD array was tested at 10 kWth for 20 min with stable responses on every channel. Measurement error is depicted in the shaded region for each data set.

Table 2
The stable detector response over 20 min for each channel was used in conjunction with the measured fissile mass which was deposited onto each sample to determine an average mass-normalized count-rate at 10 kWth for the experiment with a threshold setting of 15 for all channels.

Channel	1 (top)	2	3	4 (bottom)
Mass normalized response (cps/µg U)	235 ± 18.4	241 ± 15.3	433 ± 33.8	213 ± 7.59

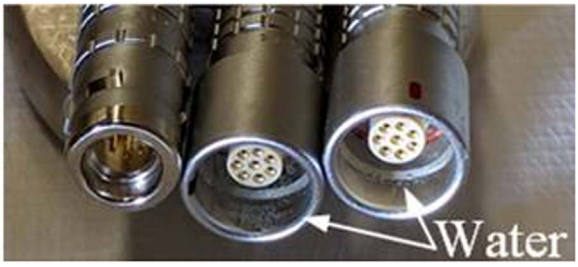

Fig. 13. The Lemo FGG/PHG.1 K.308 assembly was not entirely water-tight. The penetration of water into the electrical plug produced sufficient conductivity to degrade the MPFD signal.

discriminator setting was too low for channel 3. Additional testing was required to confirm proper discriminator setting, however, testing was halted due to excessive current flow which was observed when the plug connecting the MPFD array to the extension cable began to leak water. The water leak into the plug was identified by a sharp increase in detector response rate and an increase in HVPS current draw from <0.005 µA to >10 µA. The noise signal on the oscilloscope masked neutron-induced signals.

The array was removed from the reactor core and the plug was disassembled. The entire array was re-inserted into the heating tube and re-purged. No condensation was observed in the vacuum tube, confirming that water had only leaked into the plug. Water

was observed within the mating portion of the plug as shown in Fig. 13. The plugs were dried and additional silicone sealant was applied to the mating surfaces of the plug. Additional shrink-tubing was used to seal the plug from water.

4.2. Detector response to reactor power

After repairing the water leak in the plug assembly, the purge/fill procedure was executed three times with UHPAr and the array was re-deployed into the same test location between instrumented fuel rods at the KSU TRIGA Mk. II research nuclear reactor shown in Fig. 8. The MPFD array was operated under a +200 V applied bias with the MPR-16 in 20 MeV mode, MSCF-16 gain of 5 and shaping time of 1 μs. Neutron-induced pulses triggered the digital counting system using a discriminator setting of 5 on the MSCF-16. The sensor response was observed

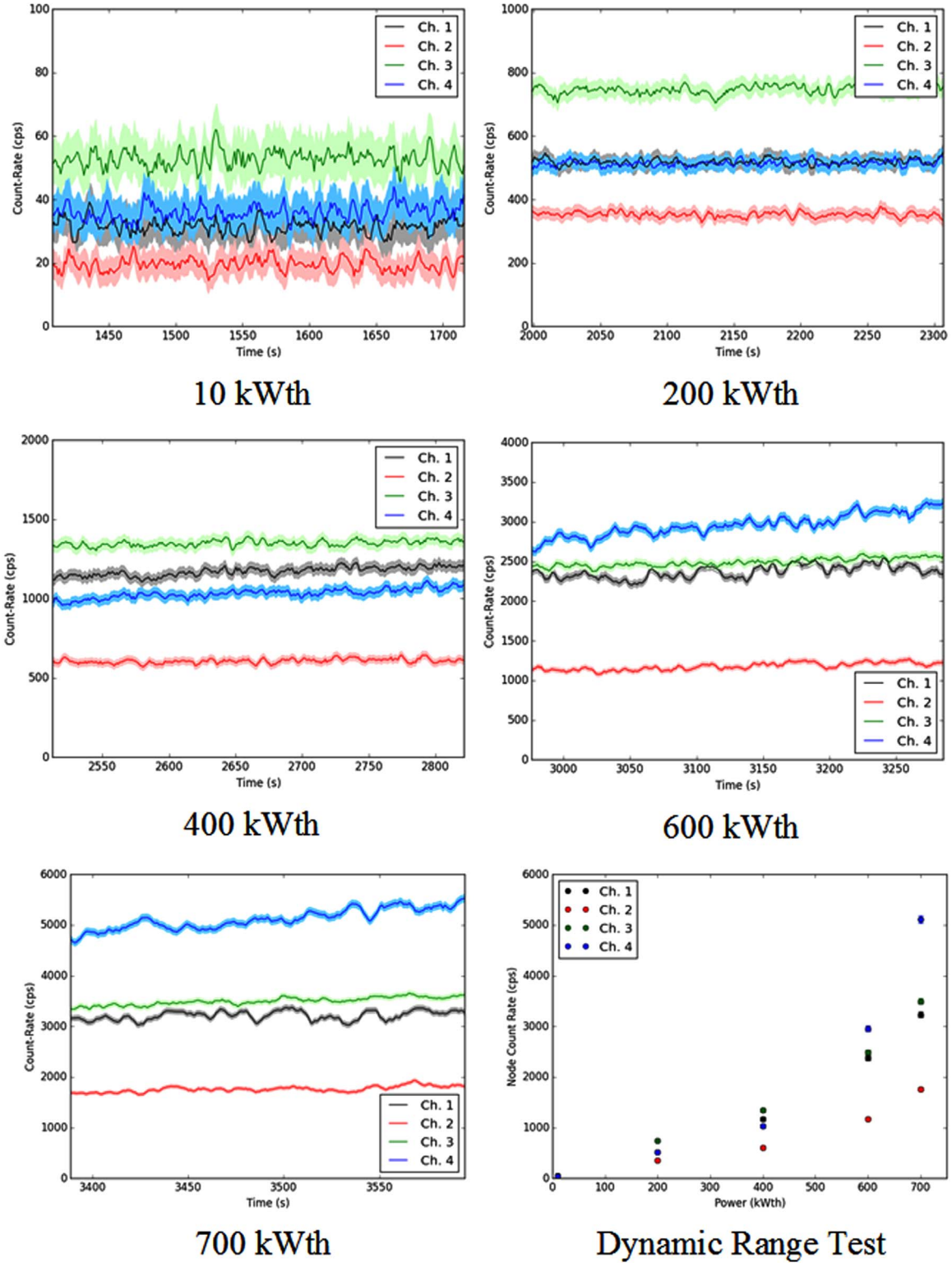

Fig. 14. All four channels of the MPFD array were tested at reactor powers of 10, 200, 400, 600, and 700 kWth. Measurement error is depicted in the shaded region for each data set.

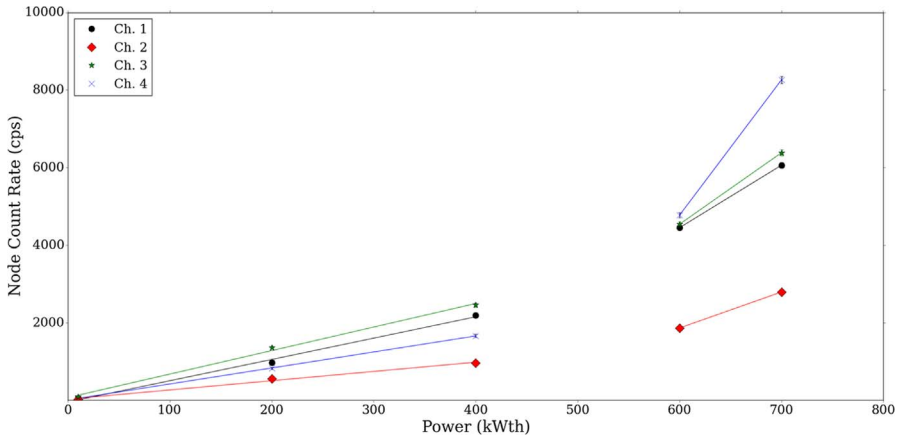

Fig. 15. The MPFD response rate was linear with power for all channels below 400 kWth, but followed a different trend above 400 kWth.

for reactor powers of 10, 200, 400, 600, and 700 kWth. Counts were summed over 5-min for each power level (2-min at 700 kWth), as shown in Fig. 14. Unlike the preliminary test results shown in Fig. 12, all four channels responded at similar rates at 10 kWth.

The detector count rate was stable on all channels for power levels of 400 kWth and below, increasing slightly with time for powers above 400 kWth. Overall, the response of each MPFD node in the array increased as the reactor power increased. The increase in detector response was linear between 10 kWth and 400 kWth for all four nodes. For reactor powers above 400 kWth, the observed signal increased slowly with time, suggesting that the local neutron flux increased even though reactor power remained constant as depicted in Fig. 15.

The two fuel elements neighboring the MPFD test location were equipped with three chromel-alumel thermocouples. The center line fuel temperature of these elements, located in the B-ring of the reactor, is recorded as the average of the three thermocouple measurements [16]. Increases in reactor local neutron flux in the instrumented fuel rods can be indicated by an increase in fuel center line temperature due to an increased rate of fission. The mass-normalized MPFD response for each node in the array was compared to the average fuel center line temperature, shown in Fig. 16. Although the response rate for nodes 2–4 increased over time at 600 kWth, the fuel center line temperature was nearly constant, suggesting that the increase in response rate was caused by another mechanism such as moderator temperature or fission poisoning. In the future, experiments should be conducted with and without reactor cooling to determine how moderator temperature affects sensor response and how that response relates to theoretical values of local neutron flux. All four MPFD channels and the fuel center line temperature increased over time at full power.

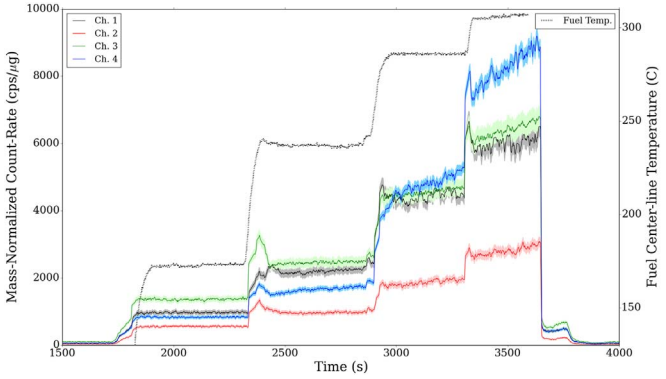

Fig. 16. The average fuel center-line temperature for the fuel elements neighboring the MPFD array remained constant at 200, 400, and 600 kWth although MPFD response rate increased over time at 600 kWth. Both the MPFD and average fuel center line temperature increase over time at full power. Measurement error is depicted in the shaded region for each data set.

4.3. Tracking reactor transients

While the 4-node encapsulated MPFD array was deployed in the reactor core, three different transient experiments were conducted to observe the capability of the MPFD array to respond to real-time changes in reactor power. First, positive reactivity insertions were observed. The rate of increase in reactor power is commonly characterized by the reactor period, the amount of time in which the reactor increased in power by a factor of *e*. First, the reactor was brought to criticality at 10 kWth using the regulating control rod while the shim control rod remained fully inserted. Then the reactor operator executed three positive reactivity insertions yielding reactor periods of approximately 30, 15, and 5 s by withdrawing the shim control rod. Maintaining a constant period requires manual operation of the control rods and was therefore only approximate. The reactor was returned to 10 kWth critical state with the shim rod fully inserted between each transient. A 1-s measurement interval was used to track real-time MPFD response on the digital counting system, shown in Fig. 17. All four detector nodes measured increasing neutron flux as the shim control rod was withdrawn. Strong effects of temperature feedback were observed, embodied by the peak in detector response followed by a sharp decline and leveling of the

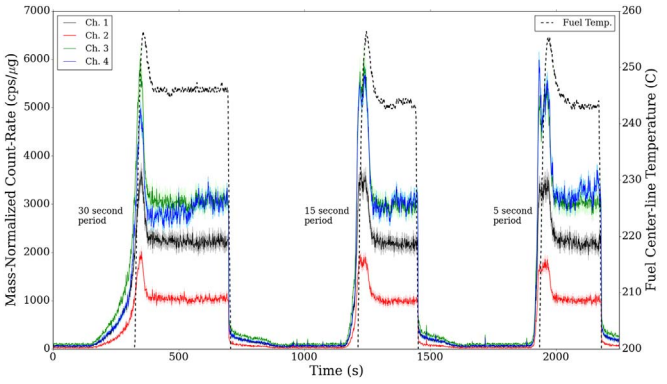

Fig. 17. Positive reactivity insertions with power periods of 30, 15, and 5 s were tracked using a 1-s counting interval illustrate the negative temperature coefficient of the fuel. Measurement error is depicted in the shaded region for each data set.

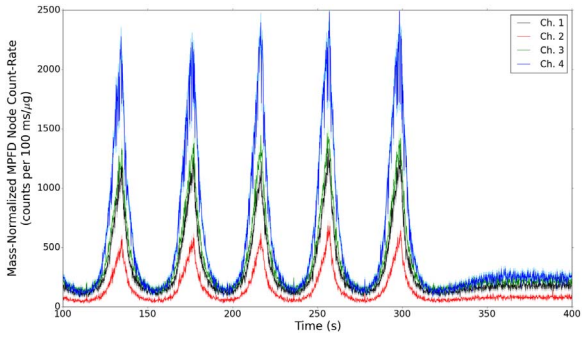

Fig. 18. Increasing and decreasing power transients were tracked using a 100-ms counting interval. Measurement error is depicted in the shaded region for each data set.

detector response and supported by the fuel temperature depicted in Fig. 17. Temperature feedback is an expected feature in a TRIGA nuclear reactor because of the negative temperature coefficient of reactivity for the reactor fuel, and was observed in previous MPFD transient tests at lower power [7].

Next, the measurement interval was decreased to 100 ms to measure manual power oscillations using the MPFD array. Reactor criticality was established at 600 kWth with the safety, shim, and pulse rod fully withdrawn and the regulating rod remained fully inserted. The regulating rod was then removed at a constant rate yielding positive reactor period of approximately 30 s until a reactor power of 900 kWth was reached. In order to prevent a linear power SCRAM triggered at 1 MWth, the reactor operator fully inserted the regulating rod reducing reactor power to the original 600 kWth level. The oscillating reactivity insertion was repeated a total of 5 times. The real-time response of all four MPFD nodes tracked the oscillation of reactor power in the core as shown in Fig. 18.

5. Conclusions

The fabrication and testing of a modular 4-node MPFD array at the KSU TRIGA Mk. II research nuclear reactor indicates the capability of such devices to be used for real-time, in-core monitoring of neutron flux in multiple locations simultaneously. However, several changes can improve the design, fabrication, and application of MPFDs. First, materials should be selected that prevent water from leaking into the electrical connections of the sensor. Also, the operating parameters must be investigated in greater detail to determine optimal operating bias, gain (for both the preamplifier and shaping amplifier), shaping time, and discriminator setting. Special attention should be given to improving the data-acquisition method for these developmental sensors in the future to further reduce sources of error in the measurements.

Acknowledgements

This paper presents work supported by the US Department of Energy Office of Nuclear Energy Contract DE-NE0008408 and U.S. Nuclear Regulatory Commission, Office of Nuclear Regulatory Research, under award number NRC-HQ-60-15-G-0004. MPFDs were fabricated in the Kansas State University Semiconductor Materials and Radiological Technologies laboratory (Manhattan, KS). Sensor testing was conducted at the Kansas State University TRIGA Mk. II research nuclear reactor facility (Manhattan, KS).

References

[1] T. Unruh, J. Rempe, D.S. McGregor, P.B. Ugorowski, M.A. Reichenberger, NEET Micro-Pocket Fission Detector - FY 2013 Status Report, Idaho National Laboratory (INL), Idaho Falls, 2013.
[2] T. Unruh, J. Daw, K. Davis, D. Knudson, J. Rempe, M. Reichenberger, P. Ugorowski, D. McGregor, J.F. Villard, Enhanced Micro Pocket Fission Detector Evaluations (Feb. 23-26), NPIC & HMIT, Charlotte, NC, 2015.
[3] T. Unruh, D. McGregor, P. Ugorowski, M. Reichenberger, T. Ito, NEET Enhanced Micro-Pocket Fission Detector for High Temperature Reactors - FY15 Status Report, Idaho National Laboratory, Idaho Falls, ID, 2015.
[4] M.F. Ohmes, D.S. McGregor, J.K. Shultis, P.M. Whaley, A.S.M.S. Ahmed, C. C. Bolinger, T.C. Pinset, Development of micro-pocket fission detectors (MPFD) for Near-core and In-core neutron flux monitoring, SPIE Proc. Hard X-Ray Gamma-Ray Detect. Phys. 5198 (2004) 234–242.
[5] D.S. McGregor, M.F. Ohmes, R.E. Ortiz, A.S.M.S. Ahmed, J.K. Shultis, Micro-pocket fission detectors (MPFD) for In-core neutron flux monitoring (*no.* A554), Nucl. Inst. Meth. (2005) 494–499.
[6] M.F. Ohmes, Micro-Pocket Fission Detector (MPFD) Development for the Kansas State University TRIGA Mark-II Nuclear Reactor (M. S. Thesis), Kansas State University, Manhattan, KS, 2006.
[7] M.A. Reichenberger, T.D.F. George, R.G. Fronk, P.B. Ugorowski, J.A. Geuther, J.A. Roberts, T. Ito, H.B. Vo-Le, S.R. Stevenson, D.M. Nichols, D.S. McGregor, "Advances in the Development and Testing of Micro-Pocket Fission Detectors (MPFDs)," in I*nternational Conference on Research Reactors: Safe Management and Effective Utilization,* Vienna, Austria, Nov. 16–20, 2015.
[8] M.A. Reichenberger, T.C. Unruh, P.B. Ugorowski, T. Ito, J.A. Roberts, S. R. Stevenson, D.M. Nichols, D.S. McGregor, Micro-Pocket Fission Detectors (MPFDs) for in-core neutron detection, Annals Nucl. Energy no. 87 (2016) 318–323.
[9] M.A. Reichenberger, T.C. Unruh, J.A. Geuther, D.M. Nichols, T.J. Sobering, J.A. Roberts, P.B. Ugorowski, D.S. McGregor, "Electronic Support System Enchnacements for Micro-Pocket Fission Detectors (MPFDs)," in Conference Proceedings IEEE Nucl. Sci. Symp., Strassbourg, FR, 2016.
[10] NucFil, LLC dba NFT, "NFT," NucFil, LLC, 2017. [Online]. Available: ⟨http://www.nftinc.com/⟩. (accessed 19 1 2017).
[11] M.A. Reichenberger, T. Ito, P.B. Ugorowski, B.W. Montag, S.R. Stevenson, D. M. Nichols, D.S. McGregor, Electrodeposition of Uranium and Thorium onto Small Platinum Electrodes, Nucl. Inst. Meth. Res. A no. 812 (2016) 12–16.
[12] M.F. Ohmes, Deployment of a Three-Dimensional Array of Micro-Pocket Fission Detector Triads for Real-Time, In-Core Neutron Flux Measurements in the Kansas State University TRIGA Mark-II Nuclear Reactor (Ph. D. Diss.), Kansas State University, Mnahattan, KS, 2012.
[13] Lemo, "FGG.1K.308.CLAK80 Specification," 11 2016. [Online]. Available: ⟨http://www.mouser.com/ds/2/232/unipole_multipole-9707.pdf⟩. (accessed 5 1 2017).
[14] Lemo, "PHG.1K.308.CLLK75 Specification," 11 2016. [Online]. Available: ⟨http://www.mouser.com/ds/2/232/unipole_multipole-9707.pdf⟩. (accessed 5 1 2017).
[15] Belden, "8134 Multi-Conductor, Low-Capacitance Computer Cable for EIA RS-232/485," 26 8 2016. [Online]. Available: ⟨http://www.belden.com/techdatas/english/8134.pdf⟩. (accessed 5 1 2017).
[16] Kansas State University, "TRIGA Mk. II Nuclear Reactor Facility Training Manual,", 2002.